Chemical Science

ROYAL SOCIETY OF CHEMISTRY

PERSPECTIVE

View Article Online
View Journal | View Issue

Cite this: *Chem. Sci.*, 2023, **14**, 11941

All publication charges for this article have been paid for by the Royal Society of Chemistry

Polymeric materials for ultrasound imaging and therapy†

Roman A. Barmin,[a] MirJavad Moosavifar,[a] Anshuman Dasgupta,[a] Andreas Herrmann,[bc] Fabian Kiessling,[a] Roger M. Pallares*[a] and Twan Lammers*[a]

Ultrasound (US) is routinely used for diagnostic imaging and increasingly employed for therapeutic applications. Materials that act as cavitation nuclei can improve the resolution of US imaging, and facilitate therapeutic US procedures by promoting local drug delivery or allowing temporary biological barrier opening at moderate acoustic powers. Polymeric materials offer a high degree of control over physicochemical features concerning responsiveness to US, *e.g. via* tuning chain composition, length and rigidity. This level of control cannot be achieved by materials made of lipids or proteins. In this perspective, we present key engineered polymeric materials that respond to US, including microbubbles, gas-stabilizing nanocups, microcapsules and gas-releasing nanoparticles, and discuss their formulation aspects as well as their principles of US responsiveness. Focusing on microbubbles as the most common US-responsive polymeric materials, we further evaluate the available chemical toolbox to engineer polymer shell properties and enhance their performance in US imaging and US-mediated drug delivery. Additionally, we summarize emerging applications of polymeric microbubbles in molecular imaging, sonopermeation, and gas and drug delivery, based on refinement of MB shell properties. Altogether, this manuscript provides new perspectives on US-responsive polymeric designs, envisaging their current and future applications in US imaging and therapy.

Received 18th August 2023
Accepted 11th October 2023

DOI: 10.1039/d3sc04339h

rsc.li/chemical-science

1. Introduction

Ultrasound (US) has a long history of use at the interface of biomedicine and materials science.[1] Depending on the operating frequencies and energies applied, US can enable material synthesis, facilitate chemical reactions, or provide diagnostic and therapeutic capabilities that can be further enhanced with the administration of responsive materials. For instance, sonication with US frequencies between 20 and 40 kHz, where substantial US intensity and US vibration amplitudes generate high shear forces, allows the synthesis of colloidal particles of different compositions.[2,3] US-assisted mechanochemistry allows chemical reactions to be enhanced or chemical bonds to be broken by combining the US-induced mechanical forces with the formation of cavitation nuclei, or the generation of reactive radicals by sonolysis.[4,5] For instance, recent examples of selective disulfide,[6–8] diselenide[9] or urea[10] bond cleavage highlight the therapeutic potential for US-assisted drug release, yet high US pulse energies and long sonication times need to be reduced to be compatible with cells and tissues.

US imaging is a diagnostic modality prevalently employed in clinical settings based on its low-cost and non-invasiveness.[11] Covering the frequency range of 2–18 MHz, US operates by emitting acoustic pulses that bounce off tissues and organs, driven by variations in acoustic impedance. These reflected signals are captured by the probe and utilized for image construction.[12] Therapeutic US encompasses frequencies between 20 kHz and 5 MHz, where focused acoustic pulses allow to temporarily open biological barriers (*i.e.*, blood–brain or skin), deliver drugs locally (*e.g.*, by destroying drug delivery systems), or even ablate tumors, depending on the settings involved.[13,14]

Materials that act as cavitation nuclei can facilitate US diagnostic and therapeutic performance.[15] For instance, the administration of contrast agents can improve the resolution of the US images by providing echogenicity greater than that of surrounding tissues, improving diagnostic capabilities for certain pathologies.[16,17] Cavitation nuclei can reduce the acoustic energies typically required for therapeutic US, as they are highly responsive to changes in pressure and temperature, resulting in rapid changes in volume and local mechanical effects required for sonopermeation and local drug delivery.[18,19] Microbubbles (MB), 1 to 5 μm-sized gas-filled vesicles, are the most commonly used agents for contrast-enhanced US imaging and cavitation, as

[a]*Institute for Experimental Molecular Imaging, RWTH Aachen University Hospital, Aachen 52074, Germany. E-mail: rmoltopallar@ukaachen.de; tlammers@ukaachen.de*

[b]*DWI – Leibniz Institute for Interactive Materials, Aachen 52074, Germany*

[c]*Institute of Technical and Macromolecular Chemistry, RWTH Aachen University, Aachen 52074, Germany*

† Electronic supplementary information (ESI) available: Polymeric material designs, applications, and the current stage of translation. See DOI: https://doi.org/10.1039/d3sc04339h

their gaseous core provides echogenicity, which is several orders of magnitude higher than that of solid particles of the same size.[18–21] Clinically available US contrast agents are based on soft, thin, and elastic lipid or protein MB shells that provide excellent oscillation profiles and strong US contrast generation.[22,23]

However, polymeric materials offer a high degree of control over their physicochemical characteristics by tailoring polymer chain properties (including monomer composition, molecular weight, hydrophobicity, stiffness) that is barely achievable with lipids or proteins. In the case of MB, polymer shells can surpass their lipid-based counterparts in several aspects. Their thicker shell can be loaded with higher amounts of drug molecules.[24,25] Their shape can be tuned, yielding anisotropic MB with better performance in drug delivery based on their increased margination behavior.[26] Moreover, their rigidity can be manipulated, improving their acoustic responses.[27] Beyond MB, polymers can facilitate the engineering of materials that stabilize the cavitation nucleus within their unique shape (as recently-demonstrated with nanocups, NC)[28] or present tailored composition with unique characteristics (as illustrated by rigid microcapsules, MC),[29,30] providing controlled acoustic responses ideally suited for US imaging and therapy.

While several insightful perspectives/reviews have been published to date focusing on different aspects of cavitation nucleation[15] and therapeutic applications of US-responsive materials,[31,32] in this perspective, we focus on recent advances in the development of polymeric materials with engineered structure and acoustic properties for US imaging and therapeutic applications. We start by providing an overview of the polymers and designs available for the construction of acoustic responsive materials. Next, we discuss the chemical tools available for tuning the polymeric MB characteristics, such as shape, shell thickness, and stiffness, and improve the flow dynamics, acoustic cavitation and drug loading capabilities of the materials. We finally highlight emerging applications of polymeric MB and discuss potential new avenues for the use of US-responsive polymeric materials for diagnosis and therapy.

2. Polymers and design features to engineer ultrasound-responsive materials

2.1. Polymers

While numerous polymers can be used for material design, a few of them are frequently used. This section and Fig. 1 highlight the most important examples of polymers used in the

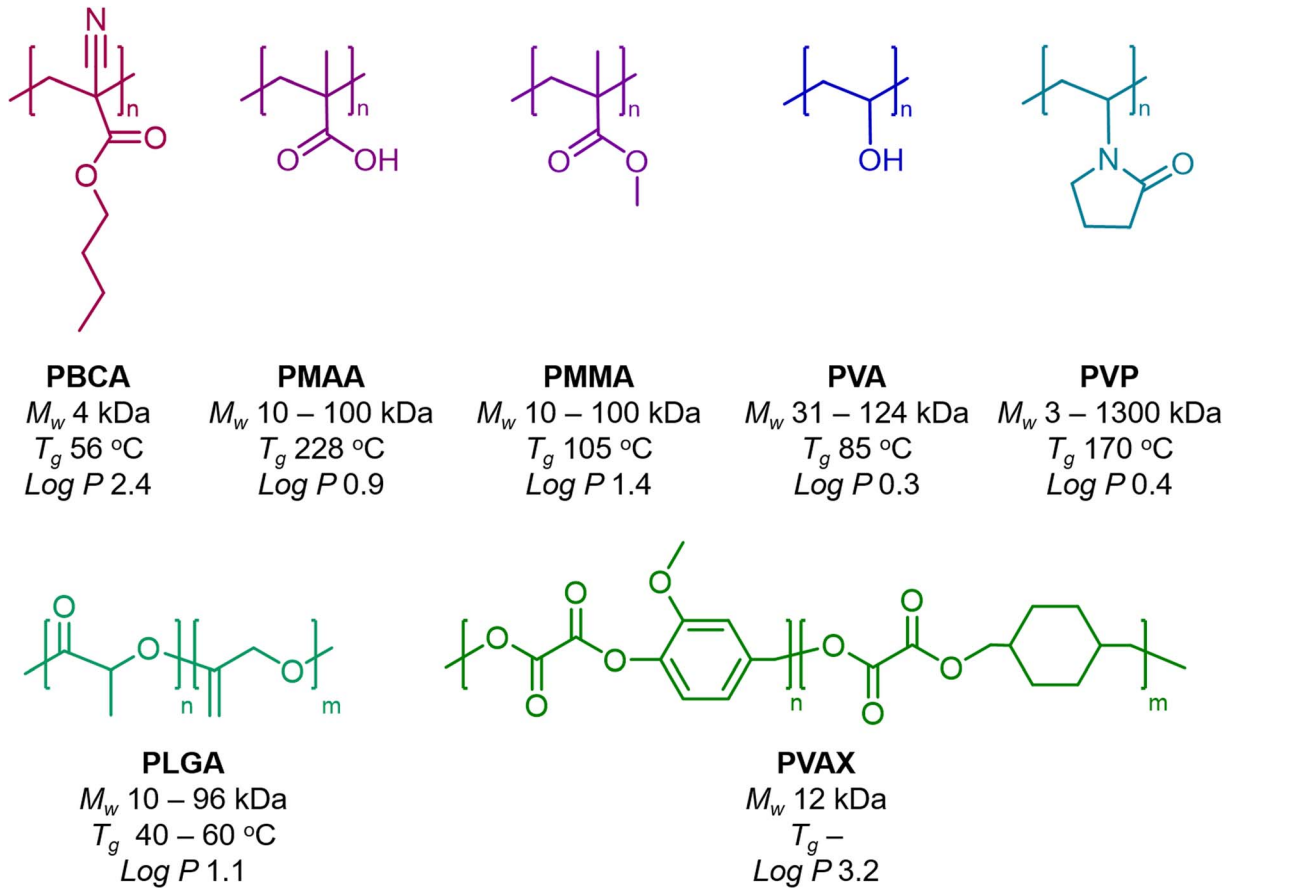

Fig. 1 Commonly used polymers for the synthesis of ultrasound-responsive materials. Chemical structures of poly(butyl cyanoacrylate) (PBCA), poly(methacrylic acid) (PMAA), poly(methyl methacrylate) (PMMA), poly(vinyl alcohol) (PVA), poly(vinyl pyrrolidone) (PVP), poly(lactic-*co*-glycolic acid) (PLGA), and poly(vanillyl alcohol-*co*-oxalate) (PVAX), as well as their properties, including molecular weights of resulting chains (M_w), glass transition temperatures (T_g), and hydrophobicity values of single monomer units (log *P*).

synthesis of polymeric materials for ultrasound imaging and therapy, with a brief description of each polymer type in a separate paragraph.

2.1.1. Poly(butyl cyanoacrylate). PBCA is a synthetic polymer approved by the U.S. Food and Drugs Administration (FDA) as surgical glue for wound closure, and widely used for MB synthesis.[33,34] PBCA MB synthesis involves the utilization of non-ionic surfactants, which serve as templates for MB formation, followed by anionic polymerization of butyl cyanoacrylate monomers to form the MB shell. The PBCA MB shells are hydrophobic (log *P* value of the monomer is 2.4), enabling them to effectively load hydrophobic drugs as payloads. The rapid polymerization of the butyl cyanoacrylate yields shells made of short PBCA chains of around 4 kDa, which are considerably below the threshold of kidney clearance (around 40 kDa).[35] The glass transition temperature (T_g) of such PBCA chains is around 56 °C, which can be later exploited in one-dimensional stretching of MB to synthesize anisotropic MB.[26]

2.1.2. Poly(methacrylic acid). PMAA is a synthetic polymer that can act as a polyelectrolyte in the synthesis of MC.[36] It possesses a pK_a value of ~4.9,[37] and consequently, the carboxylic acid groups within the polymer are predominantly deprotonated at neutral pH. Hence, the cross-linked polymer chains can swell as a function of pH in a range between 4 to 7.[38] Pre-synthesized PMAA chains of 10 to 100 kDa are extensively used during the synthesis of pH-sensitive hydrogels or layer-by-layer (LbL) coated MC, where PMAA layers are successively alternated with layers of cationic polyelectrolytes, such as poly(allylamine hydrochloride) or poly(ethylenimine). LbL coated MC can be used for US imaging, as the multilayered polymeric border can effectively scatter US waves.

2.1.3. Poly(methyl methacrylate). The methyl ester of methacrylic acid, methyl methacrylate, polymerizes to form PMMA, also known as acrylic glass.[39] In contrast to PMAA, PMMA is a tough glassy polymer with high T_g values, in the range of 85 to 165 °C, that is used in the manufacture of rigid intraocular lenses because of its transparent properties. PMMA is the main component of US-responsive NC, which are obtained by the polymerization of methyl methacrylate on top of spherical polystyrene (PS) beads in the presence of cross-linker divinylbenzene. The polymerization process induces swelling and deformation of the PS template, transforming its shape into cup-like.[28]

2.1.4. Poly(vinyl alcohol). PVA is a synthetic polymer that is "generally recognized as safe" by the FDA and approved for food packaging.[40] PVA MB are produced through the crosslinking of pre-synthesized long PVA chains, ranging from 35 to 70 kDa, in the presence of an oxidizing agent (*i.e.*, sodium periodate) under vigorous stirring.[41] Since PVA chains are hydrophilic, the functionalization strategies of PVA MB are typically based on the activation of hydroxyl groups available at the MB surface. However, the high molar mass of PVA may result in slow biodegradation rates and excretion, and significant accumulation in spleen and liver.[42,43]

2.1.5. Poly(vinyl pyrrolidone). PVP is a water-soluble synthetic polymer that is widely used as a binder in pharmaceutical tablets or antiseptic products, and is "generally recognized as safe" by the FDA.[44] The tunable range of molecular weights, which usually range from 3 to 1300 kDa, affect the viscosity of the resulting polymer. PVP can act as a polyelectrolyte, thereby, is used in the synthesis of US-responsive MC *via* LbL self-assembly, in combination with PMAA or tannic acid.[29]

2.1.6. Poly(lactic-*co*-glycolic acid). PLGA is a polymer approved by the FDA for therapeutic devices and drug delivery systems, owing to its good biodegradability and biocompatibility.[45,46] Both polymeric components provide different characteristics, since poly(lactic acid) is a hydrophobic and stiff polymer with poor mechanical strength, while poly(glycolic acid) is a hydrophilic and soft polymer with good biodegradability. Hence, by adjusting the monomer ratio between lactic and glycolic acids, the acoustic and drug loading properties (among others) of PLGA can be tuned.[47–49] Moreover, the molecular weight of the resulting polymer can also affect the payload release and dissolution kinetics of the system, since shorter chains promote faster drug release.[50–52] The synthesis of PLGA-based MB, MC and nanoparticles (NP) is based on the double emulsion solvent evaporation method.[53] It is worth noting that PVA is typically added during the synthesis in the aqueous phase as a surfactant that prevents aggregation and coalescence of the second emulsion droplets.[54] The added amount of PVA can impact the size and porosity of PLGA particles and, as a consequence, their acoustic response.[55] For instance, the presence of up to 5% of PVA during the synthesis yields single-core PLGA MB with tunable cavitation activity based on the initial PVA amount. In contrast, in the absence of PVA, PLGA MB with multiple cores that do not provide sufficient stable cavitation activity are obtained.[54]

2.1.7. Poly(vanillyl alcohol-*co*-oxalate). PVAX is the product of the copolymerization between 4-vanillyl alcohol, a vanillin derivative that is used as a food flavor, and 1,4-cyclohexanedimethanol, a low-melting solid that is employed during the esterification of polyester resins, in the presence of oxalyl chloride.[56,57] The resulting PVAX polymer shows a molecular weight of 12 kDa, and can be degraded in the presence of hydrogen peroxide, releasing carbon dioxide gas and vanillyl alcohol. NP made of PVAX are produced by single emulsification in the presence of PVA, and the release of carbon dioxide bubbles is exploited for US-based detection of hydrogen peroxide-rich muscle sites (such as injured skeletal muscles or Achilles' tendons) and the suppression of local inflammation. The high hydrophobicity of the vanillyl alcohol-*co*-oxalate unit (log *P* 3.2) endows large loading of hydrophobic drugs, as shown with curcumin-loaded PVAX NP.[57]

2.2. Design features

US contrast originates from boundaries between phases with different acoustic impedances. If the difference in acoustic impedance is small, the echogenicity is weak and the US pulses are weakly reflected. In contrast, large differences in acoustic impedance can lead to strong scattered echoes. For example, the US reflection percentage at the boundary of fat and muscles is around 1%, while the boundaries between bone and fat or soft tissues and air can yield US reflection percentages as high as 49% and 99%, respectively.[58] Hence, there are two main

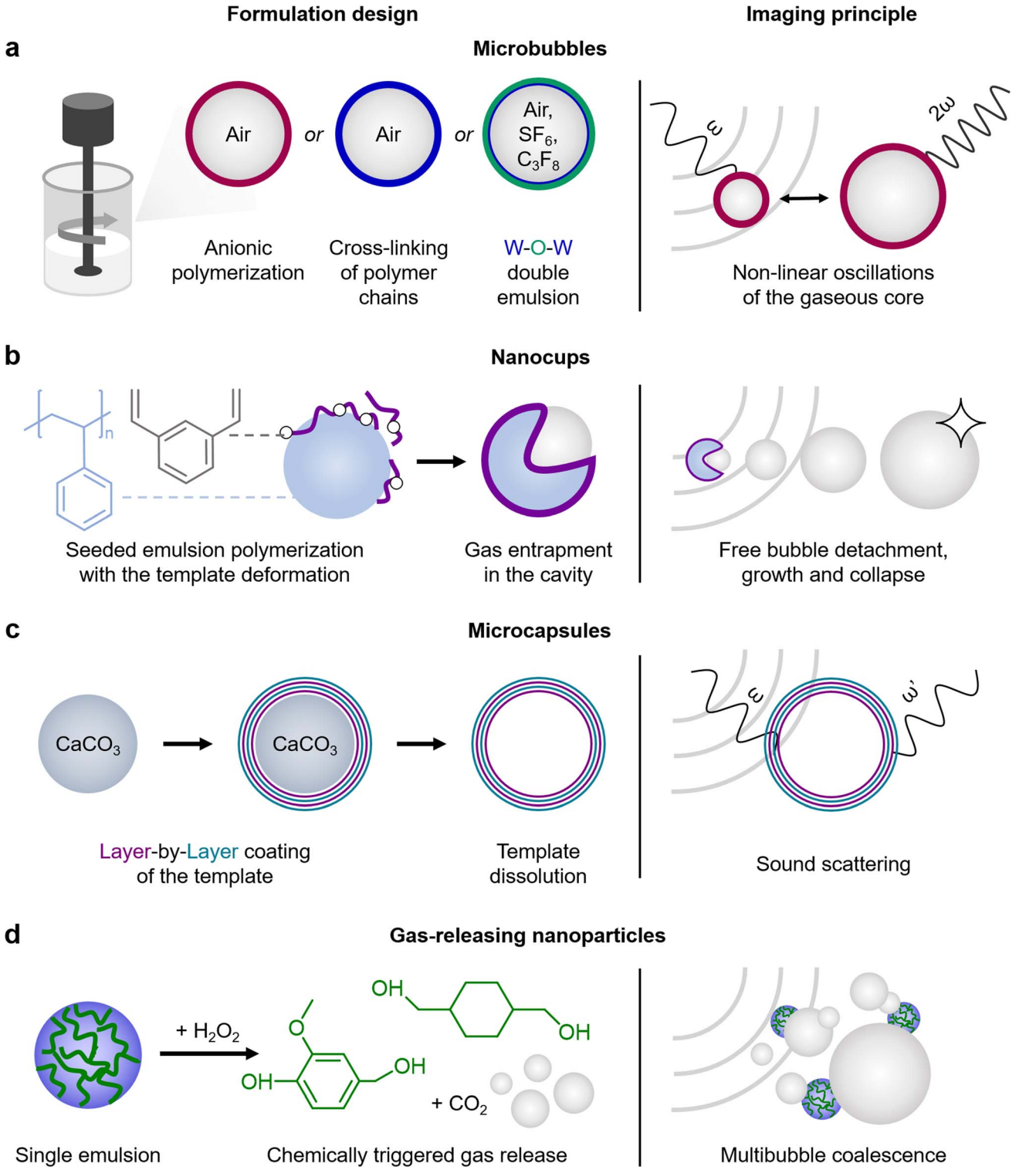

Fig. 2 Polymeric material designs and their US imaging principles. (a) Microbubbles are gas-filled vesicles with shells made of PBCA (anionic polymerization), PVA (cross-linking of PVA chains), or PLGA (by water-*in*-oil-*in*-water double emulsion). Under ultrasound pulses, gaseous cores provide non-linear oscillations, generating strong contrast signal. (b) Nanocups are produced by PMMA polymerization on the surface of poly(styrene) beads, forming hydrophobic cavities upon drying. The unstable growth and collapse of bubbles detached from the cavity of the particle provide ultrasound contrast. (c) Microcapsules are typically produced by layer-by-layer coating of templates, which may be dissolved afterwards. The multiple layer interfaces within the capsules strongly scatter US pulses. (d) Gas-releasing nanoparticles can be synthesized by single emulsion sonication, where PVAX chains are encapsulated inside the PVA nanoparticles. In the presence of a chemical trigger, such as hydrogen peroxide, PVAX dissolves into separate monomer units and releases small bubbles of carbon dioxide, which can coalesce, yielding larger bubbles with strong US contrast.

strategies to engineer polymeric materials with strong US responses: first, to stabilize a gas bubble, either by entrapping it within a shell (MB) or in a hydrophobic cavity (NC), or to generate the bubble *in situ* under specific chemical conditions (gas-releasing NP); and second, to design a rigid material with multiple boundaries with different acoustic impedances (multilayered MC).

MB are the most commonly used US contrast agents, with their shells encapsulating a gaseous core that acts as a cavitation nucleus (Fig. 2a).[15] The ability of the gaseous core to oscillate upon US pulses is dictated primarily by the shell characteristics, *e.g.* polymer elasticity. Polymeric MB show moderate US contrast compared to their lipid counterparts, yet their signal is detected by clinical US imaging settings. When the MB size is reduced to a few hundred nanometers, nanobubbles are also capable to oscillate under US pulses,[59,60] but exhibit lower echogenicity compared to MB due to the reduced volume of gas trapped inside cores. In addition, recently described polymeric nanodroplets with heavy liquid fluorocarbon-filled cores can convert into gas-filled MB upon acoustic or optical evaporation.[61–65] However, nanodroplets may require high acoustic pressures to vaporize, tend to grow significantly in size (up to several hundred microns), and burst at a certain diameter threshold, whereas MB are capable of stable cavitation at low acoustic pressures.

NC are solid polymeric nanoparticles composed of PS beads with a layer of cross-linked PMMA on top (Fig. 2b).[28] Unlike traditional spherical NP, NC exhibit unique curvatures, which result in hydrophobic cavities capable of entrapping gas. Upon US exposure, NC initiate and sustain readily detectable cavitation activity provided by the detachment of gas bubbles from the hydrophobic cavities, followed by unstable growth and collapse of the detached bubbles. It is worth noting that NC can sustain four times longer inertial cavitation *in vivo* (120 seconds) than clinically used lipid MB *SonoVue*.

Solid-shelled MC can be manufactured by LbL assembly, providing multiple phase borders within a particle, causing strong sound scattering. One approach is based on the alternating coating of PVP and PMAA or tannic acid polyelectrolyte layers on top of silica or calcium carbonate templates, followed by the template dissolution (Fig. 2c).[29] The resulting hollow LbL-coated MC display significant US contrast intensity that is comparable to *Definity* (lipid MB used in the clinic). The contrast intensity can be manipulated by the number of layers (4 or 8), the polyelectrolyte type (PMAA is less rigid than the bulky tannic acid molecule) and the polymer molecular weight (PVP of 58 kDa or 1300 kDa). Moreover, the US contrast intensities can be preserved after 6 months of storage at room temperature. LbL-coated MC also allow to use pH sensitive polyelectrolytes, such as PMAA, which swell and consequently change their US contrast intensity depending on the pH of the environment.[30]

Alternatively, polymeric NP can be engineered to release gas bubbles under specific conditions, therefore, providing US contrast relying on bubble release. Two different strategies have been developed to produce bubbles with polymeric nanoparticles. First, a nano-sized gas generator material is coated with polymers or, second, the nanoparticles themselves are synthesized with a polymer that upon degradation releases gas. As an example of the first strategy, calcium carbonate NP were coated with PLGA.[66] Calcium carbonate is stable at neutral pH, and can dissolve under acidic conditions, thereby releasing carbon dioxide gas bubbles. Since tumor microenvironments are known to be acidic (pH $\sim$ 5.5), once the NP enter the tumor site, their cores start to dissolve and generate tiny bubbles, which increase the US contrast intensity. The second strategy can be illustrated with NP formed with PVAX polymer (Fig. 2d).[56,57] Once hydrogen peroxide reacts with PVAX, the polymer disintegrates into vanillyl alcohol and carbon dioxide bubbles. Since damaged tissues in the musculoskeletal system are characterized by high hydrogen peroxide levels, these NP can be used to monitor skeletal muscle injuries and other disorders.

Other US-responsive polymeric designs include polymersomes,[67] nanovesicles,[68] micelles,[69,70] and hydrogels.[71,72] While their ability to generate detectable acoustic signal for US imaging is limited, their US-triggered destruction or rearrangement may enhance therapeutic applications in stimulus-induced drug delivery, *e.g.* in US-mediated chemotherapy delivery and sonodynamic therapy.

3. Chemical toolbox to engineer polymeric microbubble properties

Precise control over MB characteristics, including composition, shape, shell thickness, and stiffness, can improve MB performance in diagnostics as well as expand their use towards new therapeutic applications. For instance, functional US imaging requires MB formulations with soft, thin, and elastic shells in order to provide strong cavitation profiles. An increase in the available surface binding area and a well-defined bioconjugation toolbox can improve the performance of targeted MB formulations for molecular imaging. US-assisted drug delivery requires thick and rigid MB that can be loaded with large amounts of pharmaceutics and can be easily broken upon US pulses to promote drug release. Moreover, highly resilient and elastic MB are favored for sonopermeation of the blood–brain barrier, since elastic MB can sustain stable cavitation for prolonged periods of time without bursting, preventing lesions to the brain due to shell fragmentation.

3.1. MB shape

We recently discovered shape as a new physicochemical property in the MB landscape (Fig. 3a). Anisotropic MB were generated by one-dimension stretching of spherical PBCA MB embedded in PVA films, heated above the T_g of PBCA chains, and followed by cooling down to room temperature.[26] Compared to their spherical counterparts, anisotropic PBCA MB with an aspect ratio of 2.5 showed (i) two-fold increased margination behavior, as rod flow dynamics move the anisotropic MB closer to the vasculature walls, (ii) prolonged circulation times *in vivo* since rod-shaped MB showed reduced macrophage uptake, and (iii) enhanced blood–brain barrier

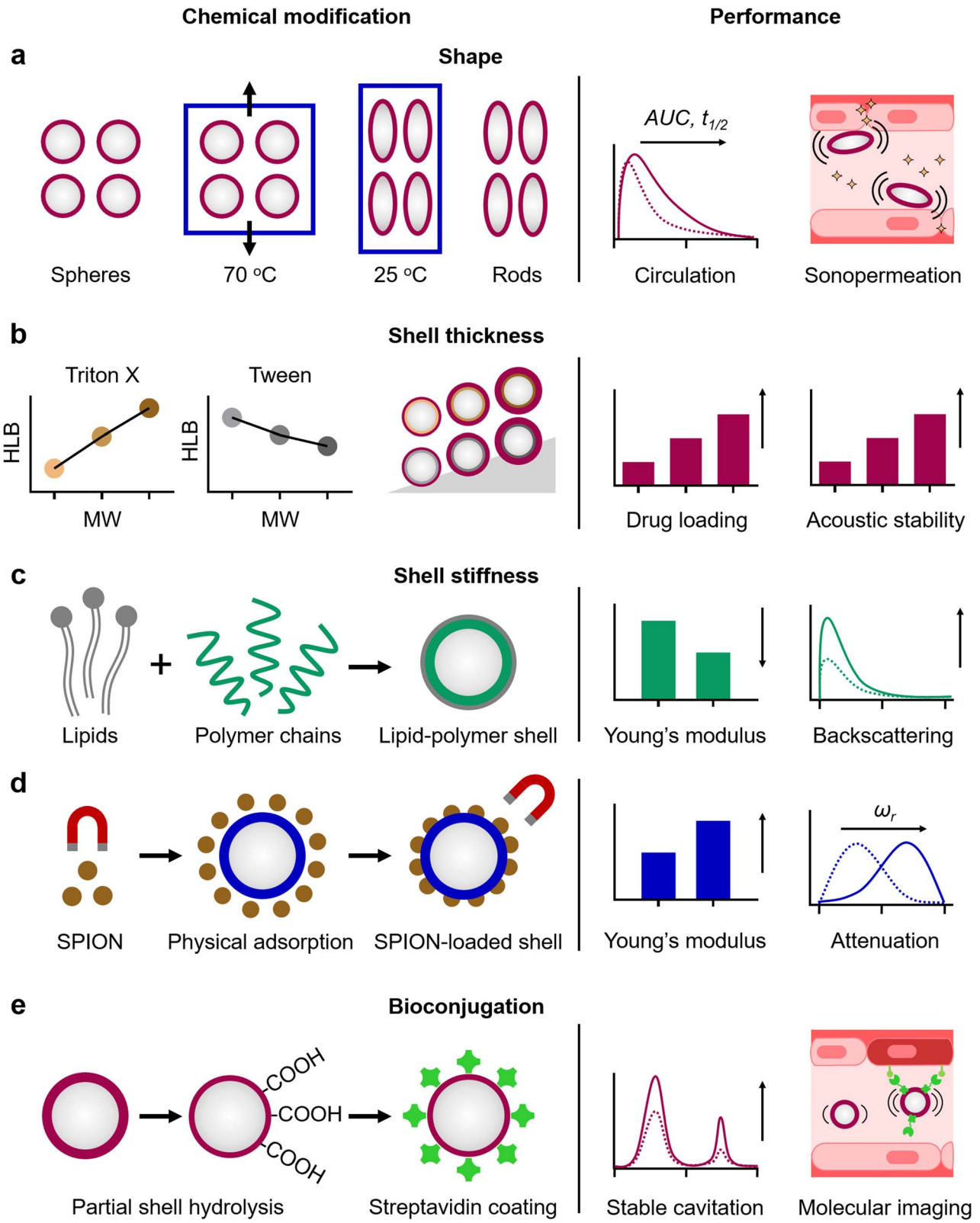

Fig. 3 Chemical toolbox to engineer polymeric microbubble properties. (a) MB shape can be manipulated by one-dimensional stretching of spherical PBCA MB embedded in PVA films at temperatures above their glass transition, followed by cooling to room temperature. Rod-shaped MB exhibit better circulation profiles (with increased areas under the curves (AUC) and circulation half-lives ($t_{1/2}$)) and strong margination propensity, consequently improving sonopermeation in comparison to their spherical counterparts. (b) Shell thickness of PBCA MB can be increased with high-molecular weight non-ionic surfactants (like Triton X and Tween) during the MB synthesis. Thicker-shelled MB provide greater drug loading capabilities and acoustic stability than thin-shelled ones. (c) Shell stiffness of PLGA MB can be manipulated by introducing soft lipids during MB synthesis, yielding a hybrid lipid-polymer shell. The resulting MB display decreased Young's modulus, thereby promoting

permeation *in vivo* upon focused US irradiation, as they generate shear forces upon oscillation closer to the endothelium barrier.

3.2. MB shell thickness

The shell thickness of polymeric MB can be engineered by controlling the polymerization rate through tuning the synthetic conditions, *e.g.* emulsification speed and selection of additives, providing thick MB shells with high drug payload capabilities and high acoustic stability (Fig. 3b). For instance, increasing the molecular weight of surfactants from Triton X and Tween families used during the synthesis of PBCA MB resulted in up to three-fold thicker MB shells.[25] Surprisingly, the higher proportion of smaller polymer chains of the Triton X-based MB, as compared to those of obtained with Tween surfactants, yielded lower polymer entanglement, improving drug loading capacity and US contrast response.

3.3. MB shell stiffness

Another key factor determining the polymeric MB acoustic responses is shell stiffness. Polymeric MB vibrate rather than oscillate under US pulses compared to the easily expandable and compressible lipid MB.[73–75] Nevertheless, the polymeric shell stiffness can be tuned by the MB composition (Fig. 3c). For example, the introduction of small portion of lipids into the PLGA MB shell yielded hybrid lipid–PLGA MB with greater elasticity than plain ones (*i.e.* Young's modulus values of 3 GPa and 5 GPa for hybrid and plain PLGA MB, respectively), and as a consequence, enhanced backscattered US signal *in vivo*.[27] Moreover, the longer circulation times of the MB formulations, combined with the spatiotemporal control over drug release, resulted in better therapeutic outcomes compared to free drug treatments. US-mediated drug delivery with doxorubicin loaded lipid–PLGA MB to achieved 86% tumor inhibitory rate compared to ~60% tumor inhibition for doxorubicin alone and increased survival time of mice with 4T1 tumor xenograft up to 46 days compared with 36 days for the untreated group. Alternatively, the physical adsorption of inorganic NP on the polymeric MB shells or their loading inside can also increase the shell stiffness and provide additional functional capabilities dictated by the inorganic NP (Fig. 3d). For example, superparamagnetic iron oxide NP physically adsorbed on PVA MB increased the shell stiffness by three-fold (0.26 N m^{-1} compared to 0.08 N m^{-1} for plain PVA MB of similar diameters), and provided magnetic properties to the US-responsive MB.[76] Furthermore, attenuation spectroscopy measurements showed that MB with stiffer shells (loaded with NP) displayed resonance frequencies at higher frequency ranges compared to plain ones (18–20 MHz and 12–14 MHz, respectively).

3.4. MB bioconjugation

Thick polymeric shells can be functionalized with biomolecules for molecular imaging and targeted drug delivery. For example, direct covalent conjugation of ligands is possible through the carboxyl groups of PBCA MB (after partial shell hydrolysis), the hydroxyl groups of PVA MB, and the carbonyl groups of PLGA MB. Alternatively, the MB shell can be functionalized with a biotin–avidin pair. Based on the targeting ligand, functionalized MB can selectively bind with endothelial cells expressing markers of atherosclerosis, angiogenesis or inflammation.[33,77,78] In addition to provide targeting capabilities, bioconjugation also impacts (and potentially improves) the MB acoustic behavior (Fig. 3e). For example, partial shell hydrolysis and subsequent streptavidin shell functionalization improved the stable cavitation profile and enhanced second harmonic generation of PBCA MB, since the process decreased the rigidity of the MB shell.[79]

4. Emerging applications of polymeric microbubbles

4.1. Advances in US imaging

Clinical US imaging devices are typically optimized for lipid and protein MB. The increased rigidity of polymeric MB, however, results in higher resonance frequencies (8 to 13 MHz) compared to their lipid and protein counterparts (4 to 5 MHz). Consequently, novel algorithms and tools are being developed to incorporate the unique characteristics of polymeric MB to US imaging. As an example, a novel contrast pulse sequence was developed for PVA MB.[80] In order to highlight the non-linear oscillations of MB, US imaging devices employ different signal processing techniques to suppress linear signals of soft tissues. Most common techniques rely on pulse inversion, amplitude modulation and measurement of subharmonics or ultraharmonics. The latter new method combines pulse inversion with subharmonics and ultraharmonics to maximize the detection of non-linear responses of MB, while reducing the background noise from soft tissues. In another study, a spatial resolution of approximately 10 μm was achieved by post-processing US image data of PBCA MB using motion model US localization microscopy (mULM). This approach improved spatial resolution by (at least) 4-fold compared to conventional US imaging approaches. This algorithm relies on locating and tracking individual MB across multiple frames of a US cineloop. mULM enables the determination of blood flow velocity and direction in microvasculature, as well as provides super-resolution images of the blood vessel network using standard clinical and preclinical US imaging devices (Fig. 4a).[81]

greater acoustic backscattering and increased ultrasound contrast intensity as compared to plain PLGA MB. (d) Shell stiffness of PVA MB can be manipulated by physical adsorption of superparamagnetic iron oxide nanoparticles (SPION) on the shell, providing magnetic capabilities to the MB. Greater rigidity (Young's modulus) of the resulting shells can shift the MB resonance frequencies (ω_r) towards higher ranges compared to plain PVA MB. (e) PBCA MB can be biofunctionalized by partial shell hydrolysis and subsequent streptavidin conjugation. Streptavidin-coated MB display enhanced stable cavitation profile compared to plain PBCA MB, while the attachment of targeting ligands through carboxyl groups or biotin–avidin pairs can be used for molecular imaging.

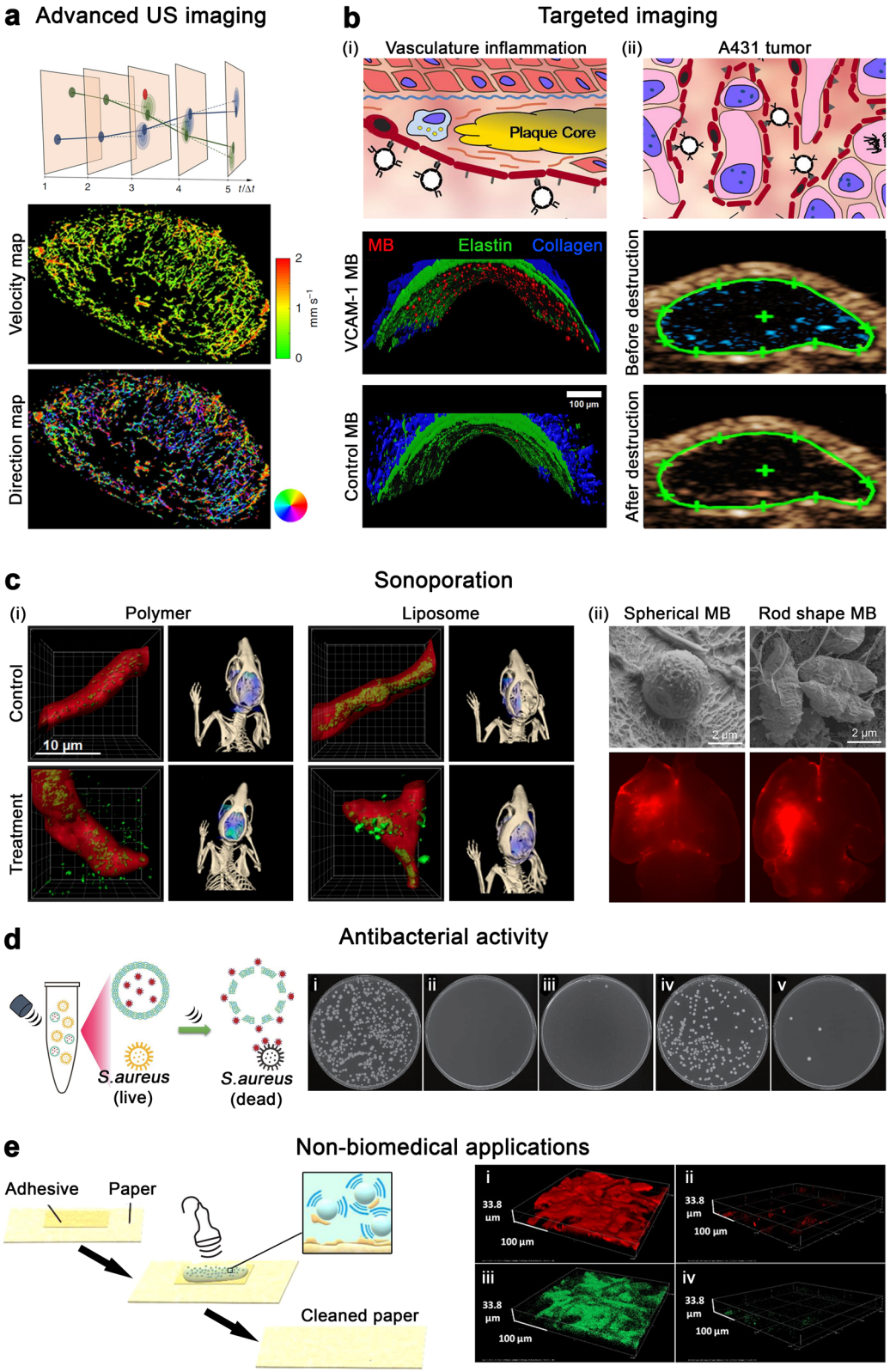

Fig. 4 Emerging applications of polymeric microbubbles. (a) A431 tumor vascular network's velocity map and direction map determined with mULM. Adapted with permission of ref. 81. Copyright 2023 Springer Nature. (b) (i) Schematic depiction of targeting MB for contrast-enhanced US imaging of endothelial biomarkers in atherosclerosis, and binding of VCAM-1-targeting MB and control MB. (ii) Illustration of molecular imaging of angiogenesis biomarkers with E-selectin targeting MB, and molecular US imaging with MB targeting E-selectin in subcutaneous A431 xenograft tumors before and after destructive US pulses. Adapted with permission of ref. 33. Copyright 2017 Elsevier. (c) (i) Microscopic and tomographic images of 10 nm polymer and 100 nm liposome accumulation in the brain of healthy mice upon sonopermeation with PBCA MB and control. Adapted with permission of ref. 89. Copyright 2020 Ivyspring International. (ii) Cryo-scanning electron micrographs of spherical and

4.2. Molecular imaging and targeted drug delivery

The thick shell of polymeric MB and the presence of functional groups on their surface enable MB decoration for targeted applications.[82,83] For instance, antibodies targeting vascular cell adhesion molecule 1 (VCAM-1, a protein overexpressed by endothelial cells during inflammation) and IELLQAR peptides targeting E-selectin (an angiogenesis marker) have been conjugated to MB and successfully used to target atherosclerosis and A431 tumor, respectively, in a mouse model (Fig. 4b).[33] Similarly, P-selectin conjugated MB were obtained by coupling fucoidan to dextran-coated polymeric MB, enabling the detection of venous thrombus in a rat model.[84] The polymeric shell can also be loaded with functional materials, such as iron oxide nanoparticles, which act as contrast agents for magnetic resonance imaging (MRI) and endow magnetic guidance of MB. For example, PBCA MB loaded with iron oxide NP and functionalized with the RGDfK peptide, which bind to $\alpha_v\beta_3$ integrin, were used to target and detect tumor microvasculature with both US and MRI.[78] In comparison to traditional small-molecule contrast agents, which extravasate from leaky blood vessels of tumors and are rapidly cleared by the kidneys, MB can remain in the vasculature for prolonged periods of time, allowing better targeting and (potentially) providing better MRI imaging of tumor vasculature. In addition, US/MRI agents can be used in interventional procedures by initially locating the lesion with whole body MRI and then using US real-time feedback to guide tumor biopsy. Alternatively, polymeric MB can be combined with more complex systems yielding biomimetic formulations with multiple functionalities. For instance, PLGA MB have been coated with platelet membranes for the detection of myocardial ischemia-reperfusion injuries.[85] The MB formulation exploited platelet targeting capabilities, immune system evasion, and sub-endothelial adhesion to image the myocardial injuries at early stages. Lastly, while conventional contrast-enhanced US diagnostics rely on the use of a single formulation, multiple MB can be used for multiplex imaging. For example, a recent study has exploited the different acoustic behavior between lipid and polymeric MB to image two biomarkers in a single systemic administration. The new US imaging method was based on the sequential collapse of $\alpha_v\beta_3$-targeting lipid MB and VEGFR2-targeting lipid-PLGA MB under different acoustic pressures to selectively image the biomarkers.[86]

4.3. Therapeutic gas release

Polymeric MB can serve as gas delivery agents for therapeutic purposes, either by filling the core with a clinically relevant gas or by loading the shell with a gas generator. For example, the cores of PVA MB were filled with nitric oxide gas, which could be locally released through US to inhibit platelet aggregation.[87] Alternatively, dimanganese decacarbonyl loaded PBCA MB were developed as responsive carbon monoxide generators. Upon light irradiation, the MB locally produced and released carbon monoxide gas, which could be used to diminish tissue damage and inflammation induced by hypoxia and reactive oxygen species. In addition, the gradual release of carbon monoxide could be detected by MRI.[88] It is worth noting that for certain applications, the amount of gas loaded in the MB cores may not be large enough to trigger physiological reactions, and consequently, the use of gas generators may be preferred.

4.4. BBB sonopermeation

Under US irradiation, polymeric MB can sustain both stable and inertial cavitation, which have been used to locally enhance perfusion of drugs across biological barriers (known as sonopermeation or sonoporation). For example, PBCA MB have been successfully utilized to deliver small and large model drugs (10 nm poly(*N*-(2-hydroxypropyl) methacrylamide) polymers and 100 nm liposomes) through the blood–brain barrier of healthy mice (Fig. 4c).[89] While both model drugs crossed through the blood–brain barrier upon sonopermeation treatment, 10 nm polymer had the highest accumulation inside the brain. Hence, this study demonstrated that sonoporation efficiency is dependent on the carrier size. Recently, MB shape has been shown to produce a significant impact on BBB sonopermeation. Rod-shaped PBCA MB, which are produced as described in detail in Section 3, have shown improved sonopermeation effects based on their extended circulation times in the bloodstream (due to lower macrophage uptake) and their tumbling effect, which locates them closer to the blood vessel walls (Fig. 4c).[26] Sonopermeation with polymeric MB can be further improved by replacing the air in the core by another (heavier) gas. For instance, compared to air, C_3F_8 is a higher molecular weight gas that shows lower water solubility. C_3F_8-filled PLGA MB displayed longer circulation times and extended cavitation profiles than their air-filled counterparts. The high duration and low intensity cavitation of C_3F_8-filled PLGA MB enabled efficient sonoporation, while avoiding permanent damage to brain tissue.[54]

4.5. Other US-induced therapeutic applications

US-responsive agents offer a promising solution for efficient and localized antibacterial activity. In cases such as chronic wounds, ulcers, or lung infections, where bacterial biofilms are formed, traditional antibiotics often have reduced effectiveness due to limited drug penetration. The cavitation of MB has the potential to disrupt biofilms and enhance the delivery of

rod shaped PBCA MB, and *ex vivo* fluorescence imaging of a mouse brain after sonoporation with the MB. Adapted with permission of ref. 26. Copyright 2023 National Academy of Science. (d) Schematic representation of *in situ* US-triggered antibacterial drug release against *S. aureus* and photographs of agar Petri dishes that were incubated with *S. aureus* containing (i) buffer (ii) vancomycin, (iii) vancomycin and gold nanoparticles, (iv) vancomycin gold nanoparticles embedded in polymeric microcapsules without sonication and (v) vancomycin gold nanoparticles embedded in polymeric microcapsules with sonication. Adapted with permission of ref. 91. Copyright 2023 Springer Nature. (e) Schematic representation of adhesive removal from paper with polymeric MB. 3D confocal laser scanning microscopy of adhesive residuals on a paper sample (i and iii) before treatment and (ii and iv) after treatment. Adapted with permission of ref. 98. Copyright 2021 American Chemical Society.

antibiotics to deeper layers, as demonstrated with lipid formulations.[90] While the use of polymeric MB for antibacterial applications is still an incipient field, other US-responsive formulations, such as silica MC containing vancomycin-modified gold nanoparticles, have demonstrated to be efficient antimicrobial agents against *S. aureus* (Fig. 4d).[91] Considering the greater cavitation response of polymeric MB, it is expected that they would exhibit significantly higher antibacterial effect than MC.

In addition, MB have recently attracted interest for enhancing the transdermal permeation of drugs (*e.g.*, the anti-inflammatory drug diclofenac), where US pulses can stimulate MB bursting that promotes deeper penetration of the drug into the skin.[92,93] MB-induced cavitation may endow its use in sonothrombolysis by improving clot disruption and reperfusion of the surrounding microvasculature compared to US alone.[94,95] The ease of shell modification and greater additive loading capabilities of polymeric MB may also facilitate their use in gene delivery.[96]

4.6. Beyond biomedical applications

The thick and formable shell of polymeric microbubbles, as compared to the more elastic lipid-based ones, provides unique possibilities for shell modification aimed at different non-medical applications. For instance, the optical features of PVA microbubbles can be tuned by inducing non-uniform shell thickness during the UV crosslinking step. This tunable coloration feature makes them potentially suitable for optical applications such as displays, sensors, and anti-counterfeiting materials.[97] In another study, PVA MB were used to remove synthetic adhesives from papers by exposing the surfaces to MB and irradiating them with 1 MHz US wave (Fig. 4e).[98]

5. Conclusion

In the last decade, interest in US has largely increased, as new diagnostic and therapeutic applications are being developed. These require the use of agents that can provide enhanced US contrast, generate additional shear forces to facilitate sonopermeation, and/or be loaded with pharmaceutics. Strong US contrast responses can be generated by stabilizing gas bubbles, either within a shell (MB) or in a hydrophobic cavity (NC), by releasing bubbles upon a chemical trigger (gas-releasing NP), and by combining multiple rigid boundaries with different acoustic impedances (multilayered MC). Polymers are commonly used to develop such US-sensitive materials, because of the wide range of parameters that can be adjusted, including polymer chain length (promoting a reasonable biodegradation rate of the formulations), glass transition temperature (regulating the stiffness of the resulting materials), and hydrophobicity (providing cavities for hydrophobic drug loading).

We here discuss micro- and nanoscale polymeric materials with US responsiveness, highlighting their formulation aspects and principles of US contrast. Because gas-filled MB are routinely used as US contrast agents, in the second half of the perspective, we focus on the available chemical toolbox to engineer polymeric MB shell properties, including shape, thickness, stiffness, and bioconjugation profile, adjusting their performance in (functional and molecular) US imaging and US-mediated therapy (drug delivery and sonopermeation). Based on the refined properties of polymeric MB, we summarize recent biomedical applications in imaging and therapeutic gas and drug delivery. The high degree of control over the physicochemical properties of polymeric MB provides them with controllable acoustic response and high drug loading capabilities that cannot be matched by their lipid- and protein-coated counterparts. This offers the potential to create finely tuned polymeric MB for desired applications: *e.g.*, ideally elastic and resilient MB for US imaging and BBB sonopermeation, where MB could cavitate without bursting, or highly brittle and thick-shelled MB for US-mediated drug delivery, where MB could maximize their drug loading and burst upon US pulses in the region of interest. By evaluating polymeric materials with tailored acoustic responses, we believe our perspective will help to inform the current status of the field and identify future research opportunities to unravel the full potential of US.

Author contributions

F. Kiessling and T. Lammers are co-founders of SonoMAC GmbH, which produces polymeric microbubbles. F. Kiessling is a consultant of Fujifilm Visualsonics.

Conflicts of interest

There are no conflicts to declare.

Acknowledgements

This work is funded by the Federal Ministry of Education and Research (BMBF), by the Ministry of Culture and Science of the German State of North Rhine-Westphalia under the Excellence Strategy of the Federal Government and the Länder through the RWTH Junior Principal Investigator (JPI) fellowship scheme, by the European Research Council (ERC CoG 864121, Meta-Targeting), the European Commission (EuroNanoMed-III: NSC4DIPG), and the German Research Foundation (DFG: GRK 2375 (grant #331065168) and SFB 1066).

References

1 S. Mitragotri, Healing sound: the use of ultrasound in drug delivery and other therapeutic applications, *Nat. Rev. Drug Discovery*, 2005, **4**, 255–260.
2 H. Xu, B. W. Zeiger and K. S. Suslick, Sonochemical synthesis of nanomaterials, *Chem. Soc. Rev.*, 2013, **42**, 2555–2567.
3 J. Nicolas, S. Mura, D. Brambilla, N. Mackiewicz and P. Couvreur, Design, functionalization strategies and biomedical applications of targeted biodegradable/biocompatible polymer-based nanocarriers for drug delivery, *Chem. Soc. Rev.*, 2013, **42**, 1147–1235.

4 T. G. McKenzie, F. Karimi, M. Ashokkumar and G. G. Qiao, Ultrasound and Sonochemistry for Radical Polymerization: Sound Synthesis, *Chem.–Eur. J.*, 2019, **25**, 5372–5388.
5 D. Yildiz, R. Göstl and A. Herrmann, Sonopharmacology: controlling pharmacotherapy and diagnosis by ultrasound-induced polymer mechanochemistry, *Chem. Sci.*, 2022, **13**, 13708–13719.
6 Z. Shi, Q. Song, R. Göstl and A. Herrmann, Mechanochemical activation of disulfide-based multifunctional polymers for theranostic drug release, *Chem. Sci.*, 2021, **12**, 1668–1674.
7 S. Huo, P. Zhao, Z. Shi, M. Zou, X. Yang, E. Warszawik, M. Loznik, R. Göstl and A. Herrmann, Mechanochemical bond scission for the activation of drugs, *Nat. Chem.*, 2021, **13**, 131–139.
8 M. Xuan, J. Fan, V. N. Khiêm, M. Zou, K.-O. Brenske, A. Mourran, R. Vinokur, L. Zheng, M. Itskov, R. Göstl and A. Herrmann, Polymer Mechanochemistry in Microbubbles, *Adv. Mater.*, 2023, 2305130.
9 T. Kharandiuk, K. H. Tan, W. Xu, F. Weitenhagen, S. Braun, R. Göstl and A. Pich, Mechanoresponsive diselenide-crosslinked microgels with programmed ultrasound-triggered degradation and radical scavenging ability for protein protection, *Chem. Sci.*, 2022, **13**, 11304–11311.
10 Y. Tong, M. Li, H. Huang, S. Long, W. Sun, J. Du, J. Fan, L. Wang, B. Liu and X. Peng, Urea-Bond Scission Induced by Therapeutic Ultrasound for Biofunctional Molecule Release, *J. Am. Chem. Soc.*, 2022, **144**, 16799–16807.
11 R. Anne, L. Wiltrud, T. Benjamin, L. Twan, M. Chrit, S. Georg and K. Fabian, Advanced Ultrasound Technologies for Diagnosis and Therapy, *J. Nucl. Med.*, 2018, **59**, 740.
12 P. N. T. Wells, Ultrasound imaging, *Phys. Med. Biol.*, 2006, **51**, R83.
13 D. L. Miller, N. B. Smith, M. R. Bailey, G. J. Czarnota, K. Hynynen, I. R. S. Makin and M. Bioeffects, Committee of the American Institute of Ultrasound in, Overview of Therapeutic Ultrasound Applications and Safety Considerations, *J. Ultrasound Med.*, 2012, **31**, 623–634.
14 N. Güvener, L. Appold, F. de Lorenzi, S. K. Golombek, L. Y. Rizzo, T. Lammers and F. Kiessling, Recent advances in ultrasound-based diagnosis and therapy with micro- and nanometer-sized formulations, *Methods*, 2017, **130**, 4–13.
15 E. Stride and C. Coussios, Nucleation, mapping and control of cavitation for drug delivery, *Nat. Rev. Phys.*, 2019, **1**, 495–509.
16 D. Cosgrove, Ultrasound contrast agents: An overview, *Eur. J. Radiol.*, 2006, **60**, 324–330.
17 F. Kiessling, S. Fokong, J. Bzyl, W. Lederle, M. Palmowski and T. Lammers, Recent advances in molecular, multimodal and theranostic ultrasound imaging, *Adv. Drug Delivery Rev.*, 2014, **72**, 15–27.
18 F. Kiessling, S. Fokong, P. Koczera, W. Lederle and T. Lammers, Ultrasound microbubbles for molecular diagnosis, therapy, and theranostics, *J. Nucl. Med.*, 2012, **53**, 345–348.
19 K. Kooiman, H. J. Vos, M. Versluis and N. de Jong, Acoustic behavior of microbubbles and implications for drug delivery, *Adv. Drug Delivery Rev.*, 2014, **72**, 28–48.
20 S. Kunjachan, J. Ehling, G. Storm, F. Kiessling and T. Lammers, Noninvasive Imaging of Nanomedicines and Nanotheranostics: Principles, Progress, and Prospects, *Chem. Rev.*, 2015, **115**, 10907–10937.
21 P. G. Rudakovskaya, R. A. Barmin, P. S. Kuzmin, E. P. Fedotkina, A. N. Sencha and D. A. Gorin, Microbubbles Stabilized by Protein Shell: From Pioneering Ultrasound Contrast Agents to Advanced Theranostic Systems, *Pharmaceutics*, 2022, **14**, 1236.
22 A. Upadhyay and S. V. Dalvi, Microbubble Formulations: Synthesis, Stability, Modeling and Biomedical Applications, *Ultrasound Med. Biol.*, 2019, **45**, 301–343.
23 J. Mujtaba, J. Liu, K. K. Dey, T. Li, R. Chakraborty, K. Xu, D. Makarov, R. A. Barmin, D. A. Gorin, V. P. Tolstoy, G. Huang, A. A. Solovev and Y. Mei, Micro-Bio-Chemo-Mechanical-Systems: Micromotors, Microfluidics, and Nanozymes for Biomedical Applications, *Adv. Mater.*, 2021, **33**, e2007465.
24 M. C. Cochran, J. Eisenbrey, R. O. Ouma, M. Soulen and M. A. Wheatley, Doxorubicin and paclitaxel loaded microbubbles for ultrasound triggered drug delivery, *Int. J. Pharm.*, 2011, **414**, 161–170.
25 R. A. Barmin, A. Dasgupta, C. Bastard, L. De Laporte, S. Rütten, M. Weiler, F. Kiessling, T. Lammers and R. M. Pallares, Engineering the Acoustic Response and Drug Loading Capacity of PBCA-Based Polymeric Microbubbles with Surfactants, *Mol. Pharm.*, 2022, **19**(9), 3256–3266.
26 A. Dasgupta, T. Sun, R. Palomba, E. Rama, Y. Zhang, C. Power, D. Moeckel, M. Liu, A. Sarode, M. Weiler, A. Motta, C. Porte, Z. Magnuska, A. Said Elshafei, R. Barmin, A. Graham, A. McClelland, D. Rommel, E. Stickeler, F. Kiessling, R. M. Pallares, L. De Laporte, P. Decuzzi, N. McDannold, S. Mitragotri and T. Lammers, Nonspherical ultrasound microbubbles, *Proc. Natl. Acad. Sci. U. S. A.*, 2023, **120**, e2218847120.
27 Y. Chen, Y. Liang, P. Jiang, F. Li, B. Yu and F. Yan, Lipid/PLGA Hybrid Microbubbles as a Versatile Platform for Noninvasive Image-Guided Targeted Drug Delivery, *ACS Appl. Mater. Interfaces*, 2019, **11**, 41842–41852.
28 J. J. Kwan, R. Myers, C. M. Coviello, S. M. Graham, A. R. Shah, E. Stride, R. C. Carlisle and C. C. Coussios, Ultrasound-Propelled Nanocups for Drug Delivery, *Small*, 2015, **11**, 5305–5314.
29 J. Chen, S. Ratnayaka, A. Alford, V. Kozlovskaya, F. Liu, B. Xue, K. Hoyt and E. Kharlampieva, Theranostic Multilayer Capsules for Ultrasound Imaging and Guided Drug Delivery, *ACS Nano*, 2017, **11**, 3135–3146.
30 J. A.-T. Walker, X. Wang, K. Peter, K. Kempe and S. R. Corrie, Dynamic Solid-State Ultrasound Contrast Agent for Monitoring pH Fluctuations In Vivo, *ACS Sens.*, 2020, **5**, 1190–1197.

31 R. Chandan, S. Mehta and R. Banerjee, Ultrasound-Responsive Carriers for Therapeutic Applications, *ACS Biomater. Sci. Eng.*, 2020, **6**, 4731–4747.
32 P. Wei, E. J. Cornel and J. Du, Ultrasound-responsive polymer-based drug delivery systems, *Drug Delivery Transl. Res.*, 2021, **11**, 1323–1339.
33 P. Koczera, L. Appold, Y. Shi, M. Liu, A. Dasgupta, V. Pathak, T. Ojha, S. Fokong, Z. Wu, M. Van Zandvoort, O. Iranzo, A. J. C. Kuehne, A. Pich, F. Kiessling and T. Lammers, PBCA-based polymeric microbubbles for molecular imaging and drug delivery, *J. Controlled Release*, 2017, **259**, 128–135.
34 P. Couvreur, (Poly-cyanoacrylate) nanomedicines for cancer and beyond: Lessons learned, *J. Controlled Release*, 2021, **334**, 318–326.
35 L. Appold, Y. Shi, S. Rütten, A. Kühne, A. Pich, F. Kiessling and T. Lammers, Physicochemical Characterization of the Shell Composition of PBCA-Based Polymeric Microbubbles, *Macromol. Biosci.*, 2017, **17**, 1700002.
36 A. N. Zelikin, A. D. Price and B. Städler, Poly(Methacrylic Acid) Polymer Hydrogel Capsules: Drug Carriers, Sub-compartmentalized Microreactors, Artificial Organelles, *Small*, 2010, **6**, 2201–2207.
37 J. P. Best, M. P. Neubauer, S. Javed, H. H. Dam, A. Fery and F. Caruso, Mechanics of pH-Responsive Hydrogel Capsules, *Langmuir*, 2013, **29**, 9814–9823.
38 L. Ruiz-Pérez, A. Pryke, M. Sommer, G. Battaglia, I. Soutar, L. Swanson and M. Geoghegan, Conformation of Poly(methacrylic acid) Chains in Dilute Aqueous Solution, *Macromolecules*, 2008, **41**, 2203–2211.
39 U. Ali, K. J. B. A. Karim and N. A. Buang, A Review of the Properties and Applications of Poly(Methyl Methacrylate) (PMMA), *Polym. Rev.*, 2015, **55**, 678–705.
40 C. C. DeMerlis and D. R. Schoneker, Review of the oral toxicity of polyvinyl alcohol (PVA), *Food Chem. Toxicol.*, 2003, **41**, 319–326.
41 L. Oddo, B. Cerroni, F. Domenici, A. Bedini, F. Bordi, E. Chiessi, S. Gerbes and G. Paradossi, Next generation ultrasound platforms for theranostics, *J. Colloid Interface Sci.*, 2017, **491**, 151–160.
42 B. Cerroni, R. Cicconi, L. Oddo, M. Scimeca, R. Bonfiglio, R. Bernardini, G. Palmieri, F. Domenici, E. Bonanno, M. Mattei and G. Paradossi, *In vivo* biological fate of poly(vinylalcohol) microbubbles in mice, *Heliyon*, 2018, **4**, e00770.
43 Å. A. Barrefelt, T. B. Brismar, G. Egri, P. Aspelin, A. Olsson, L. Oddo, S. Margheritelli, K. Caidahl, G. Paradossi, L. Dähne, R. Axelsson and M. Hassan, Multimodality imaging using SPECT/CT and MRI and ligand functionalized 99mTc-labeled magnetic microbubbles, *EJNMMI Res.*, 2013, **3**, 12.
44 M. Kurakula and G. Rao, Pharmaceutical assessment of polyvinylpyrrolidone (PVP): As excipient from conventional to controlled delivery systems with a spotlight on COVID-19 inhibition, *J. Drug Delivery Sci. Technol.*, 2020, **60**, 102046.
45 S. Rezvantalab, N. I. Drude, M. K. Moraveji, N. Güvener, E. K. Koons, Y. Shi, T. Lammers and F. Kiessling, PLGA-Based Nanoparticles in Cancer Treatment, *Front. Pharmacol*, 2018, **9**, 1260.
46 O. A. Sindeeva, O. I. Gusliakova, O. A. Inozemtseva, A. S. Abdurashitov, E. P. Brodovskaya, M. Gai, V. V. Tuchin, D. A. Gorin and G. B. Sukhorukov, Effect of a Controlled Release of Epinephrine Hydrochloride from PLGA Microchamber Array: *In Vivo* Studies, *ACS Appl. Mater. Interfaces*, 2018, **10**, 37855–37864.
47 R. A. Miller, J. M. Brady and D. E. Cutright, Degradation rates of oral resorbable implants (polylactates and polyglycolates): Rate modification with changes in PLA/PGA copolymer ratios, *J. Biomed. Mater. Res.*, 1977, **11**, 711–719.
48 F. Alexis, Factors affecting the degradation and drug-release mechanism of poly(lactic acid) and poly[(lactic acid)-*co*-(glycolic acid)], *Polym. Int.*, 2005, **54**, 36–46.
49 H. K. Makadia and S. J. Siegel, Poly Lactic-*co*-Glycolic Acid (PLGA) as Biodegradable Controlled Drug Delivery Carrier, *Polymers*, 2011, **3**, 1377–1397.
50 G. Mittal, D. K. Sahana, V. Bhardwaj and M. N. V. Ravi Kumar, Estradiol loaded PLGA nanoparticles for oral administration: Effect of polymer molecular weight and copolymer composition on release behavior *in vitro* and *in vivo*, *J. Controlled Release*, 2007, **119**, 77–85.
51 I. Mylonaki, E. Allémann, F. Delie and O. Jordan, Imaging the porous structure in the core of degrading PLGA microparticles: The effect of molecular weight, *J. Controlled Release*, 2018, **286**, 231–239.
52 M. Ochi, B. Wan, Q. Bao and D. J. Burgess, Influence of PLGA molecular weight distribution on leuprolide release from microspheres, *Int. J. Pharm.*, 2021, **599**, 120450.
53 F. Ramazani, W. Chen, C. F. van Nostrum, G. Storm, F. Kiessling, T. Lammers, W. E. Hennink and R. J. Kok, Strategies for encapsulation of small hydrophilic and amphiphilic drugs in PLGA microspheres: State-of-the-art and challenges, *Int. J. Pharm.*, 2016, **499**, 358–367.
54 S. Tsirkin, R. Goldbart, T. Traitel and J. Kost, Tailor-Made Single-Core PLGA Microbubbles as Acoustic Cavitation Enhancers for Therapeutic Applications, *ACS Appl. Mater. Interfaces*, 2021, **13**, 25748–25758.
55 I. Gupta, X. Su, U. S. Jonnalagadda, D. Das, M. Pramanik and J. J. Kwan, Investigating the Acoustic Response and Contrast Enhancement of Drug-Loadable PLGA Microparticles with Various Shapes and Morphologies, *Ultrasound Med. Biol.*, 2021, **47**, 1844–1856.
56 G.-W. Kim, C. Kang, Y.-B. Oh, M.-H. Ko, J.-H. Seo and D. Lee, Ultrasonographic Imaging and Anti-inflammatory Therapy of Muscle and Tendon Injuries Using Polymer Nanoparticles, *Theranostics*, 2017, **7**, 2463–2476.
57 E. Jung, J. Noh, C. Kang, D. Yoo, C. Song and D. Lee, Ultrasound imaging and on-demand therapy of peripheral arterial diseases using H_2O_2-Activated bubble generating anti-inflammatory polymer particles, *Biomaterials*, 2018, **179**, 175–185.
58 J. E. Aldrich, Basic physics of ultrasound imaging, *Crit. Care Med.*, 2007, **35**, S131–S137.
59 Y. Zhu, Y. Sun, W. Liu, W. Guan, H. Liu, Y. Duan and Y. Chen, Magnetic polymeric nanobubbles with optimized

core size for MRI/ultrasound bimodal molecular imaging of prostate cancer, *Nanomedicine*, 2020, **15**, 2901–2916.

60 W. Um, H. Ko, D. G. You, S. Lim, G. Kwak, M. K. Shim, S. Yang, J. Lee, Y. Song, K. Kim and J. H. Park, Necroptosis-Inducible Polymeric Nanobubbles for Enhanced Cancer Sonoimmunotherapy, *Adv. Mater.*, 2020, **32**, 1907953.

61 P. Shende and S. Jain, Polymeric nanodroplets: an emerging trend in gaseous delivery system, *J. Drug Targeting*, 2019, **27**, 1035–1045.

62 D. S. Li, S. J. Yoon, I. Pelivanov, M. Frenz, M. O'Donnell and L. D. Pozzo, Polypyrrole-Coated Perfluorocarbon Nanoemulsions as a Sono-Photoacoustic Contrast Agent, *Nano Lett.*, 2017, **17**, 6184–6194.

63 C. Mannaris, C. Yang, D. Carugo, J. Owen, J. Y. Lee, S. Nwokeoha, A. Seth and B. M. Teo, Acoustically responsive polydopamine nanodroplets: A novel theranostic agent, *Ultrason. Sonochem.*, 2020, **60**, 104782.

64 R. Melich, P. Bussat, L. Morici, A. Vivien, E. Gaud, T. Bettinger and S. Cherkaoui, Microfluidic preparation of various perfluorocarbon nanodroplets: Characterization and determination of acoustic droplet vaporization (ADV) threshold, *Int. J. Pharm.*, 2020, **587**, 119651.

65 E. A. Maksimova, D. Nozdriukhin, S. K. Kalva, S. Lyu, B. Lafci, M.-A. Augath, P. G. Rudakovskaya, A. A. Solovev, Y. Mei, X. L. Deán-Ben, D. Razansky and D. A. Gorin, Multilayer Polymer Shell Perfluoropentane Nanodroplets for Multimodal Ultrasound, Magnetic Resonance, and Optoacoustic Imaging, *Laser Photonics Rev.*, 2023, **17**, 2300137.

66 J. Lee, H.-S. Min, D. G. You, K. Kim, I. C. Kwon, T. Rhim and K. Y. Lee, Theranostic gas-generating nanoparticles for targeted ultrasound imaging and treatment of neuroblastoma, *J. Controlled Release*, 2016, **223**, 197–206.

67 P. Wei, M. Sun, B. Yang, J. Xiao and J. Du, Ultrasound-responsive polymersomes capable of endosomal escape for efficient cancer therapy, *J. Controlled Release*, 2020, **322**, 81–94.

68 K. Yang, L. Yue, G. Yu, L. Rao, R. Tian, J. Wei, Z. Yang, C. Sun, X. Zhang, M. Xu, Z. Yuan, X. Chen and R. Wang, A hypoxia responsive nanoassembly for tumor specific oxygenation and enhanced sonodynamic therapy, *Biomaterials*, 2021, **275**, 120822.

69 H. Zhang, H. Xia, J. Wang and Y. Li, High intensity focused ultrasound-responsive release behavior of PLA-*b*-PEG copolymer micelles, *J. Controlled Release*, 2009, **139**, 31–39.

70 B. Yang and J. Du, On the origin and regulation of ultrasound responsiveness of block copolymer nanoparticles, *Sci. China: Chem.*, 2020, **63**, 272–281.

71 N. Huebsch, C. J. Kearney, X. Zhao, J. Kim, C. A. Cezar, Z. Suo and D. J. Mooney, Ultrasound-triggered disruption and self-healing of reversibly cross-linked hydrogels for drug delivery and enhanced chemotherapy, *Proc. Natl. Acad. Sci. U. S. A.*, 2014, **111**, 9762–9767.

72 L. Zhu, X. Wang, M. Ding, N. Yu, Y. Zhang, H. Wu, Q. Zhang, J. Liu and J. Li, Prodrug-loaded semiconducting polymer hydrogels for deep-tissue sono-immunotherapy of orthotopic glioblastoma, *Biomater. Sci.*, 2023, **11**, 6823–6833.

73 S. H. Bloch, M. Wan, P. A. Dayton and K. W. Ferrara, Optical observation of lipid- and polymer-shelled ultrasound microbubble contrast agents, *Appl. Phys. Lett.*, 2004, **84**, 631–633.

74 D. Grishenkov, C. Pecorari, T. B. Brismar and G. Paradossi, Characterization of Acoustic Properties of PVA-Shelled Ultrasound Contrast Agents: Ultrasound-Induced Fracture (Part II), *Ultrasound Med. Biol.*, 2009, **35**, 1139–1147.

75 B. L. Helfield, X. Chen, B. Qin, S. C. Watkins and F. S. Villanueva, Mechanistic Insight into Sonoporation with Ultrasound-Stimulated Polymer Microbubbles, *Ultrasound Med. Biol.*, 2017, **43**, 2678–2689.

76 M. Poehlmann, D. Grishenkov, S. V. V. N. Kothapalli, J. Härmark, H. Hebert, A. Philipp, R. Hoeller, M. Seuss, C. Kuttner, S. Margheritelli, G. Paradossi and A. Fery, On the interplay of shell structure with low- and high-frequency mechanics of multifunctional magnetic microbubbles, *Soft Matter*, 2014, **10**, 214–226.

77 S. Fokong, A. Fragoso, A. Rix, A. Curaj, Z. Wu, W. Lederle, O. Iranzo, J. Gätjens, F. Kiessling and M. Palmowski, Ultrasound molecular imaging of E-selectin in tumor vessels using poly *n*-butyl cyanoacrylate microbubbles covalently coupled to a short targeting peptide, *Invest. Radiol.*, 2013, **48**, 843–850.

78 V. Pathak, T. Nolte, E. Rama, A. Rix, S. M. Dadfar, V. Paefgen, S. Banala, E. M. Buhl, M. Weiler, V. Schulz, T. Lammers and F. Kiessling, Molecular magnetic resonance imaging of Alpha-v-Beta-3 integrin expression in tumors with ultrasound microbubbles, *Biomaterials*, 2021, **275**, 120896.

79 R. A. Barmin, A. Dasgupta, A. Rix, M. Weiler, L. Appold, S. Rütten, F. Padilla, A. J. C. Kuehne, A. Pich, L. De Laporte, F. Kiessling, R. M. Pallares and T. Lammers, Enhanced Stable Cavitation and Nonlinear Acoustic Properties of Poly(butyl cyanoacrylate) Polymeric Microbubbles after Bioconjugation, *ACS Biomater. Sci. Eng.*, 2022, DOI: **10.1021/acsbiomaterials.2c01021**.

80 H. Chen, D. Evangelou, K. Loskutova, M. Ghorbani and D. Grishenkov, On the Development of a Novel Contrast Pulse Sequence for Polymer-Shelled Microbubbles, *IEEE Trans. Ultrason. Ferroelectrics Freq. Control*, 2021, **68**, 1569–1579.

81 T. Opacic, S. Dencks, B. Theek, M. Piepenbrock, D. Ackermann, A. Rix, T. Lammers, E. Stickeler, S. Delorme, G. Schmitz and F. Kiessling, Motion model ultrasound localization microscopy for preclinical and clinical multiparametric tumor characterization, *Nat. Commun.*, 2018, **9**, 1527.

82 P. Hauff, M. Reinhardt, A. Briel, N. Debus and M. Schirner, Molecular Targeting of Lymph Nodes with L-Selectin Ligand-specific US Contrast Agent: A Feasibility Study in Mice and Dogs, *Radiology*, 2004, **231**, 667–673.

83 M. Palmowski, J. Huppert, G. Ladewig, P. Hauff, M. Reinhardt, M. M. Mueller, E. C. Woenne, J. W. Jenne, M. Maurer, G. W. Kauffmann, W. Semmler and F. Kiessling, Molecular profiling of angiogenesis with

targeted ultrasound imaging: early assessment of antiangiogenic therapy effects, *Mol. Cancer Ther.*, 2008, **7**, 101–109.

84 B. Li, R. Aid-Launais, M.-N. Labour, A. Zenych, M. Juenet, C. Choqueux, V. Ollivier, O. Couture, D. Letourneur and C. Chauvierre, Functionalized polymer microbubbles as new molecular ultrasound contrast agent to target P-selectin in thrombus, *Biomaterials*, 2019, **194**, 139–150.

85 L. Xu, Y. Chen, Q. Jin, Y. Wu, C. Deng, Y. Zhong, L. Lin, L. Chen, W. Fu, L. Yi, Z. Sun, X. Qin, Y. Li, Y. Yang and M. Xie, Biomimetic PLGA Microbubbles Coated with Platelet Membranes for Early Detection of Myocardial Ischaemia-Reperfusion Injury, *Mol. Pharm.*, 2021, **18**, 2974–2985.

86 Z. Li, M. Lai, S. Zhao, Y. Zhou, J. Luo, Y. Hao, L. Xie, Y. Wang and F. Yan, Ultrasound Molecular Imaging for Multiple Biomarkers by Serial Collapse of Targeting Microbubbles with Distinct Acoustic Pressures, *Small*, 2022, **18**, 2108040.

87 F. Cavalieri, I. Finelli, M. Tortora, P. Mozetic, E. Chiessi, F. Polizio, T. B. Brismar and G. Paradossi, Polymer Microbubbles As Diagnostic and Therapeutic Gas Delivery Device, *Chem. Mater.*, 2008, **20**, 3254–3258.

88 V. Pathak, K. Roemhild, S. Schipper, N. Groß-Weege, T. Nolte, S. Ruetten, E. M. Buhl, A. El Shafei, M. Weiler, L. Martin, G. Marx, V. Schulz, F. Kiessling, T. Lammers and P. Koczera, Theranostic Trigger-Responsive Carbon Monoxide-Generating Microbubbles, *Small*, 2022, **18**, 2200924.

89 J. N. May, S. K. Golombek, M. Baues, A. Dasgupta, N. Drude, A. Rix, D. Rommel, S. von Stillfried, L. Appold, R. Pola, M. Pechar, L. van Bloois, G. Storm, A. J. C. Kuehne, F. Gremse, B. Theek, F. Kiessling and T. Lammers, Multimodal and multiscale optical imaging of nanomedicine delivery across the blood–brain barrier upon sonopermeation, *Theranostics*, 2020, **10**, 1948–1959.

90 F. Plazonic, G. LuTheryn, C. Hind, M. Clifford, M. Gray, E. Stride, P. Glynne-Jones, M. Hill, J. M. Sutton and D. Carugo, Bactericidal Effect of Ultrasound-Responsive Microbubbles and Sub-inhibitory Gentamicin against Pseudomonas aeruginosa Biofilms on Substrates With Differing Acoustic Impedance, *Ultrasound Med. Biol.*, 2022, **48**, 1888–1898.

91 J. Fan, M. Xuan, P. Zhao, M. Loznik, J. Chen, F. Kiessling, L. Zheng and A. Herrmann, Ultrasound responsive microcapsules for antibacterial nanodrug delivery, *Nano Res.*, 2023, **16**, 2738–2748.

92 A. H. Liao, H. Y. Chung, W. S. Chen and M. K. Yeh, Efficacy of Combined Ultrasound-and-Microbubbles-Mediated Diclofenac Gel Delivery to Enhance Transdermal Permeation in Adjuvant-Induced Rheumatoid Arthritis in the Rat, *Ultrasound Med. Biol.*, 2016, **42**, 1976–1985.

93 S. Shao, S. Wang, L. Ren, J. Wang, X. Chen, H. Pi, Y. Sun, C. Dong, L. Weng, Y. Gao and L. Wang, Layer-by-Layer Assembly of Lipid Nanobubbles on Microneedles for Ultrasound-Assisted Transdermal Drug Delivery, *ACS Appl. Bio Mater.*, 2022, **5**, 562–569.

94 M. de Saint Victor, C. Crake, C. C. Coussios and E. Stride, Properties, characteristics and applications of microbubbles for sonothrombolysis, *Expert Opin. Drug Delivery*, 2014, **11**, 187–209.

95 M. de Saint Victor, L. C. Barnsley, D. Carugo, J. Owen, C. C. Coussios and E. Stride, Sonothrombolysis with Magnetically Targeted Microbubbles, *Ultrasound Med. Biol.*, 2019, **45**, 1151–1163.

96 M. Cochran and M. A. Wheatley, In vitro gene delivery with ultrasound-triggered polymer microbubbles, *Ultrasound Med. Biol.*, 2013, **39**, 1102–1119.

97 H. Chen, H. Zhu, Y. Wang, J. Liu, Y. Wang, X. Hu, A. A. Solovev, G. Huang and Y. Mei, Structural Coloration by Internal Reflection and Interference in Hydrogel Microbubbles and Their Precursors, *Adv. Opt. Mater.*, 2021, **9**, 2100259.

98 A. D'Andrea, L. Severini, F. Domenici, S. Dabagov, V. Guglielmotti, D. Hampai, L. Micheli, E. Placidi, M. Titubante, C. Mazzuca, G. Paradossi and A. Palleschi, Ultrasound-Stimulated PVA Microbubbles for Adhesive Removal from Cellulose-Based Materials: A Groundbreaking Low-Impact Methodology, *ACS Appl. Mater. Interfaces*, 2021, **13**, 24207–24217.